Hindawi
Shock and Vibration
Volume 2018, Article ID 8252815, 11 pages
https://doi.org/10.1155/2018/8252815

Research Article

Double-Target Switching Control of Vehicle Longitudinal Low-Frequency Vibration Based on Fuzzy Logic

Donghao Hao,[1] **Changlu Zhao**,[1] **Ying Huang**,[1] **Peilin Dai**,[1] **and Yongjian Liu**[2]

[1]*Research Center of Power Machinery, School of Mechanical Engineering, Beijing Institute of Technology, Beijing 100081, China*
[2]*Delphi Shanghai Dynamics and Propulsion Systems Co. Ltd., Shanghai 200131, China*

Correspondence should be addressed to Ying Huang; hy111@bit.edu.cn

Received 15 August 2018; Revised 15 October 2018; Accepted 24 October 2018; Published 2 December 2018

Academic Editor: José J. Rangel-Magdaleno

Rapid increase of vehicle longitudinal acceleration is required in an engine torque increasing phase, whereas little overshoot and oscillating acceleration are required in a torque holding phase. These two features give satisfying results with respect to both drivability and comfortability. However, when subjected to a sudden torque change in the tip-in condition, the driveline undergoes strong low-frequency torsional vibration which has an adverse impact on vehicle comfortability. Normally, a linear quadratic (LQ) controller has a good comfort performance in reducing the vibration but with negative impact on the dynamic response of the vehicle which weakens the drivability. The two different performance demands in the two phases cannot be achieved simultaneously by only adjusting the weighting coefficients of the LQ controller. Therefore, a new control strategy decoupling the two phases is necessary and proposed in this paper. A linear quadratic regulator (LQR) is used in the torque increasing phase for dynamic response demand while a linear quadratic tracking (LQT) controller is applied in the torque holding phase for comfortability demand. The two controllers are switched smoothly via a fusion weighting factor based on the proposed fuzzy logic switching strategy. A quantitative evaluation method is used to evaluate the performances of the proposed control strategy. The results show that the double-targets switching control keeps better performances in both drivability and comfortability. The comfortability index of the proposed strategy is improved by 79.74% compared with that of the LQT whereas the dynamic response index is improved by 21.88% compared with that of the LQR.

1. Introduction

Several aspects become increasingly important in the customer demands of "top of the line products," such as fuel economy, comfortability, and driveability (the difference between the vehicle handling desired by the driver and the real behavior) of vehicle. The driveability includes several aspects of the driver's perception, which are highly subjective. The focus in this paper is the longitudinal low-frequency vibration, which produces unpleasant oscillations of vehicle and negatively affects the passenger's comfort. Typical resonance frequencies are 0–10 Hz in the longitudinal direction mainly depending on the gear ratio, which are caused by the elastic parts in the vehicle driveline, such as the clutch, driveshaft, halfshaft, and tire [1]. Besides, the backlash and the low mechanical damping make the powertrain prone to oscillate more drastically [1]. The oscillations occur, in particular, adjacent to gearshifts and during tip-in and tip-out (when the driver pushes and releases the accelerator pedal rapidly) [2, 3]. To be able to damp out the vibration, several control methods are used widely in the automotive industry.

The easiest way to reduce the low-frequency oscillations is open-loop control. One typical case is to install input torque filtering and rate shaping algorithms. A zero vibration (ZV) input shaping method was proposed in which the shape timing is based on a vehicle model to damp out the oscillation on a manual transmission front wheel drive vehicle [4]. The authors compared ZV input shaping with input filtering and concluded that ZV input shaping is superior to input filtering as shock/jerk is reduced to 25%. However, both the two methods have poor responses during the initial stage of acceleration. Moreover, the open-loop control methods are implemented in automotive manufactures' engine control unit, in which the final engine output torque is queried via

lookup tables by using engine speed and acceleration pedal position as inputs. Obviously, the disadvantages are that the controller performance depends on the subjective calibration methodology and calibrator's experience. Besides, filling lookup tables for all gears, engine speed, and pedal position combinations requires a significant amount of development time. Considering these drawbacks, the subject of automated torque control based on close loop control for improving driveability is a research topic being studied by both automotive manufacturers and academic researchers. The proportional-integral-derivative (PID) controller is widely used to damp out the longitudinal vibration, but the overall performance is not satisfactory due to the fact that it cannot ensure a fast transient response [5]. A pole placement control was designed by using a simplified linear model to damp longitudinal vehicle oscillations [6]. The simulation results show that the oscillations are well damped whereas the response time and engine speed are worse. Templin developed a LQR-based driveline antijerk controller which acts as a torque compensator and does not require any state reference trajectories [7]. Fredriksson studied different linear controllers such as PID, pole placement, and linear quadratic Gaussian/loop transfer recovery (LQR/LTR) [5]. The proposed LQR/LTR controller was evaluated as the most suitable one as it is easy to tune and works satisfactorily both in simulations as well as in real field trials. Nevertheless, the transient performance becomes less clear when the penalty on the torsion increases to damp out the wheel speed oscillations. Bruce proposed the concept of using a feedforward controller in combination with a LQ feedback [8]. The feedforward loop is based on an approximate inverse plant model to provide a fast control signal compensating for the oscillatory modes. Fang involves a new model reference approach using engine speed as a control objective, letting the actual engine speed follow the reference speed calculated by a designed transfer function [9]. Compared with state space and PID controllers, it shows better performance on vibration suppression but the output torque is a bit higher than the torque limit. Due to the superior properties in coping with constraints and unmeasured disturbance, model predictive control (MPC) obtains significant interest recently in vehicle control applications. Lagerberg proposed an MPC controller with constraints on the input torque and input torque rate [10]. It achieved promising performance in powertrain vibration suppression. However, the proposed MPC controller needs high computation, and some simplifications of the model are needed such that delays are able to be ignored and all the state variables can be measured, according to the authors. Baumann also used MPC approach to minimize driveline oscillations [11]. However, the speed difference is reduced to only 50% compared to the uncontrolled system, and the longitudinal acceleration still vibrates. Baumann also designed a robust controller using loop shaping and mixed sensitivity approach to minimize the driveline oscillations and the parametric uncertainty arising due to the aging of the mechanical components [12]. Because that the essential idea of H-infinity control is to optimize the performance for the worst external input conditions, the vehicle longitudinal acceleration still remains with some oscillations.

Above all, it can be concluded that to reduce longitudinal oscillation, open-loop controls depend on the calibrator's experience and require a significant amount of development time. Although LQ-based controls are easy to tune, the conflict between the dynamic response and the comfort is not possible to reach a suitable manner. Robust controllers are able to deal with the parametric uncertainty but the acceleration still remains with some oscillations. Due to the fact that comfortability is contradictory to the dynamic response, a comprehensive control strategy is necessary, which can handle both dynamic response and comfort at the same time. In order to achieve the best compromise between the two targets, a fuzzy-based multialgorithm fusion control strategy, which combines the LQ torque regulator and LQT speed tracking controls, is proposed in this study. The basic concept of this strategy is to distribute each a local optimal torque in the two separate phases without neglecting the driver's dynamic and comfort requests. The fuzzy-based multialgorithm fusion control strategy is designed for smooth switch and distribution of torque in the two continued phases.

The article is arranged as follows. Section 2 provides a three-dimensional multibody dynamic vehicle model for close-loop verification of the proposed controller and a control-oriented vehicle model for model-based controller design. Section 3 shows the details of the LQ-based torque regulator and LQT-based speed tracking control for vehicle longitudinal oscillation reduction. The performances are analyzed and compared in this section. The algorithm's fusion mechanism, structure, and design are presented in Section 4. The performances of the proposed vibration control strategy and the comparison with the traditional control strategies are discussed in Section 5. A quantitative evaluation method is used for performances' evaluation in this section. Section 6 is the conclusion of this work.

2. The Simulation and Control-Oriented Vehicle Model

This section describes a three-dimensional multibody dynamic vehicle model for off-line verification of the proposed controller and a control-oriented vehicle model for model-based controller design.

A vehicle powertrain consists of various complex components such as a flywheel, clutch, gearbox, differential (final drive), driveshaft, wheels, and tires. These components form a high-order nonlinear system. Due to a large torque transported from the engine to the tires, the overall system cannot be treated as completely rigid, considering torsional elasticity of the dual mass flywheel, driveshaft, and backlash mechanisms, although most of the components are made from iron derivatives. Therefore, we established a three-dimensional multibody dynamic vehicle model shown in Figure 1, using multibody dynamics software ADAMS/car (MSC Software Inc.). Elastic elements include halfshafts, bushings for the engine mount, tires, springs, and shock absorbers of the suspensions. All components have six degrees of freedom. From the literatures [2, 13, 14], it can be concluded that the vehicle longitudinal low-frequency vibration is mainly caused by the coupling of the driveline torsional vibration, the

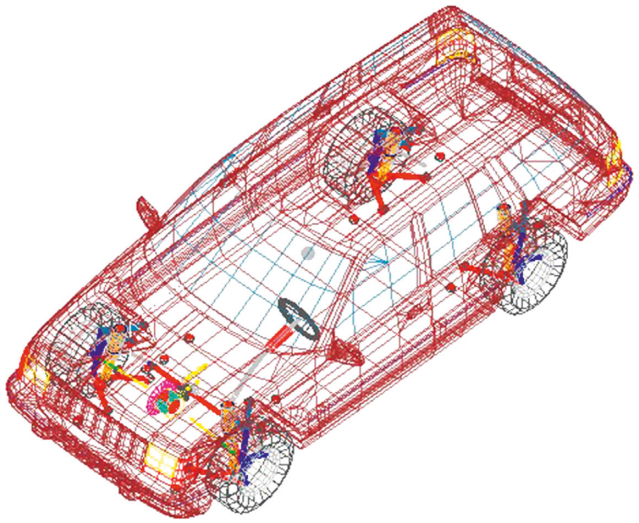

Figure 1: Three-dimensional vehicle model.

suspension vertical vibration, and the body longitudinal vibration. With this three-dimensional model, all the main influence factors of the longitudinal vibration are considered in detail. Therefore, the 3-D model is believed to reflect the complexity of a real vehicle in terms of the longitudinal vibration characteristics. The model parameters are listed in Appendix A. In order to design an advanced model-based controller, a simplified model is necessary to be able to capture the system dynamics. Several driveline and vehicle longitudinal dynamic models have been proposed in the literature, in which two mass models are the most common ones considering benefits of simplicity for running controller algorithms [15–17]. This study is based on a two mass vehicle model with the road load component for simulating longitudinal dynamics shown as Figure 2.

J_1 is the lumped rotational inertia of the engine flywheel, clutch, and gearbox shafts. J_2 is the lumped rotational inertia of the differential shaft, halfshaft, wheel hub, and vehicle. k_s and c_s are the equivalent torsional stiffness and damping coefficients of the clutch, halfshaft, and tire. i is the total transmission ratio from the engine to the wheel, which is equal to the product of the gearbox transmission ratio and differential transmission ratio. In tip-in condition, rolling resistance and air drag are small due to low speed. Thus, the vehicle load can be neglected, and T_{load} is equal to zero. The dynamic equations for the two-degree-of-freedom model are shown by the following equation:

$$\begin{aligned} J_1\ddot{\theta}_1 &= T_e + i \cdot T_s - b_1\dot{\theta}_1, \\ J_2\ddot{\theta}_2 &= T_s - T_{load} - b_2\dot{\theta}_2, \\ T_s &= k_s\left(\frac{-\theta_1}{i} + \theta_2\right) + c_s\left(\frac{-\dot{\theta}_1}{i} + \dot{\theta}_2\right), \\ a_v &= r \cdot \ddot{\theta}_2, \end{aligned} \tag{1}$$

where θ_1 is the rotational angle of the engine flywheel, θ_2 is the equivalent rotational speed of the vehicle which is equal to the wheel speed neglecting the tire slip, T_e is the engine

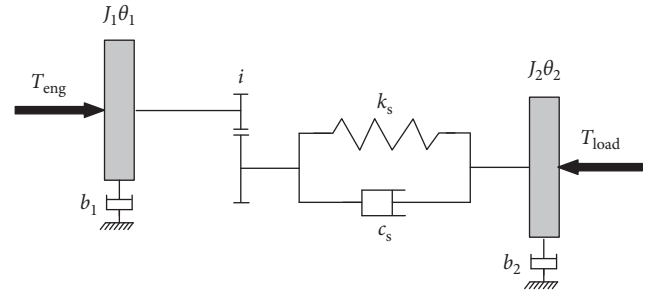

Figure 2: Two-dof control-oriented vehicle model.

effective output torque, a_v is the longitudinal acceleration of the vehicle, and r is the tire effective radius. The dynamic equations are converted to a state-space formulation by the following equation:

$$\begin{aligned} \dot{X} &= AX + Bu, \\ Y &= CX + Du, \end{aligned} \tag{2}$$

where

$$\begin{aligned} A &= \begin{bmatrix} \frac{-2c_s - i^2b_1}{i^2J_1} & \frac{2c_s}{iJ_1} & \frac{-2k_s}{iJ_1} \\ \frac{2c_s}{iJ_2} & \frac{-2c_s - b_2}{J_2} & \frac{2k_s}{J_2} \\ \frac{1}{i} & -1 & 0 \end{bmatrix}, \\ B &= \begin{bmatrix} \frac{1}{J_1} & 0 & 0 \end{bmatrix}^T, \\ C_R &= \begin{bmatrix} \frac{-c_s}{i} & c_s & -k_s \end{bmatrix}, \\ C_T &= \begin{bmatrix} 1 & 0 & 0 \end{bmatrix}, \\ D &= 0, \\ X &= \begin{bmatrix} \dot{\theta}_1 & \dot{\theta}_2 & \frac{\theta_1}{i} - \theta_2 \end{bmatrix}, \end{aligned} \tag{3}$$

where $\dot{\theta}_1$ is equal to the rotational speed of the engine flywheel, $\dot{\theta}_2$ is equal to the wheel speed, $\theta_1/i - \theta_2$ is equal to the angle difference between the engine flywheel and the wheel, C_R is the output matrix for LQR control design, and C_T is the output matrix for LQT control design. Parameters in the two degree-of-freedom model are identified by comparing the state values with that of the three-dimensional vehicle model by using the least square method [13]. The state-space model is used in the next section for the LQR and LQT controller design.

3. Torque Regulating and Speed Tracking Controls

3.1. Torque Regulating. The longitudinal vibration will be suppressed if the halfshaft torque varies smoothly which will result a stable road drive force with less oscillation. Therefore, the vibration control problem can be described as

minimizing the derivative of the halfshaft torque [18] but with a little change in engine torque as cost. An advantage with this choice is that no reference trajectories are needed for the implementation of the final control law since the reference value for the derivative of the halfshaft torque should be always zero. This can be formulated in a cost criterion consisting of two terms. The first term describes the derivative of the halfshaft torque. The second term describes the deviation in the control signal from the current level to zero which means that the controller output follows the driver's torque request. Besides, integral action is introduced by extending the model by a fourth state x_u that integrates the difference between the driver's demand torque and the controller output. This ensures that the controller output asymptotically follows the driver's torque demand. The cost function is described by the following equation:

$$J = \frac{1}{2}\int_0^\infty \left(y^T Q y + (u - u_r)^2\right) dt, \tag{4}$$

where the system output is defined by $y(t) = [\dot{T}_s \ \dot{x}_u]^T$, Q is the diagonal positive semidefinite 2×2 weighting matrix, $u(t)$ is the final engine output torque applied on driveline, and u_r is the driver's engine torque demand. The trade-off between rise time and control signal amplitude is controlled by tuning the matrix Q. Equation (4) needs to be reformulated in order to derive the optimal control law to minimize it by the standard method. Define a steady-state solution X_r such that

$$0 = AX_r + Bu_r \Longrightarrow X_r = -A^{-1}Bu_r. \tag{5}$$

Then, the new states and input of the reformulated state space equation are defined by the following equation:

$$\begin{aligned} X_n &= \begin{bmatrix} X - X_r \\ x_u \end{bmatrix}, \\ u_n &= u - u_r. \end{aligned} \tag{6}$$

The transformed system then becomes

$$\begin{aligned} \dot{X}_n &= \begin{bmatrix} A & 0 \\ 0 & 0 \end{bmatrix} X_n + \begin{bmatrix} B \\ 1 \end{bmatrix} u_n \\ &= A_n X_n + B_n u_n, \\ y &= \begin{bmatrix} C_R A & 0 \\ 0 & 1 \end{bmatrix} X_n + \begin{bmatrix} C_R B \\ 0 \end{bmatrix} u_n \\ &= C_n X_n + D_n u_n. \end{aligned} \tag{7}$$

Then, Equation (4) can be rewritten as follows:

$$\begin{aligned} J &= \frac{1}{2}\int_0^\infty \left(y^T Q y + u_n^2\right) \\ &= \frac{1}{2}\int_0^\infty \begin{bmatrix} X_n^T & u_n \end{bmatrix} \begin{bmatrix} C_R^T Q C_R & C_R^T Q D_n \\ D_n^T Q C_R & 1 + D_n^T Q D_n \end{bmatrix} \begin{bmatrix} X_n \\ u_n \end{bmatrix} dt \\ &= \frac{1}{2}\int_0^\infty \begin{bmatrix} X_n^T & u_n \end{bmatrix} \begin{bmatrix} Q_n & S \\ S^T & R \end{bmatrix} dt. \end{aligned} \tag{8}$$

By using the solved P in Equation (8), the feedback control gain is obtained by

$$K_{(1\times 4)} = R^{-1}\left(B_n^T P + S^T\right) = \frac{B_n^T P + S^T}{1 + D_n^T Q D_n}, \tag{9}$$

due to

$$u_n = -K_{(1\times 4)} X_n = -K_{(1\times 3)}\left(X - X_r\right) - K_{(1\times 1)} x_u. \tag{10}$$

The original controller output is calculated by the following equation:

$$\begin{aligned} u &= -K_{(1\times 3)} X - K_{(1\times 1)} x_u + \left(-K_{(1\times 3)} X_r\right) \\ &= -K_{(1\times 3)} X - K_{(1\times 1)} x_u + \left(1 - K_{(1\times 3)} A^{-1} B\right) u_r. \end{aligned} \tag{11}$$

From Equation (11), it can be concluded that the control law is the sum of a linear weighting of the states X and x_u as well as a feed-forward term from the driver's torque demand u_r. The weighting factors in the matrix Q are fixed in the whole time range, which means it makes a global optimal solution. In that case, we can only get a compromise between comfort and dynamic response. However, the actual requirement is that a sharp rising torque is needed in the torque rising phase within less than 0.1 s whereas a suppressed vibration is needed in the torque holding phase. The global optimal solution is not able to strictly meet the different requirements in these two separate phases simultaneously. Besides, the performance of the LQR-based torque regulator control is shown in the last part of that section, compared with that of the LQT-based control designed in the next part.

3.2. Speed Tracking. A reference model of vehicle longitudinal dynamic is needed to produce the tracking signal. For the equipped sensors in a vehicle, the engine speed is easy to be captured from the CAN bus, and the resolution is higher than that of the wheel speed. Therefore, a reference engine speed is obtained by a two-inertia rigid vehicle model which neglects all the flexible parts in the driveline [19]. The input is the demand torque from the driver's acceleration pedal. In this case, the cost function is described by the following equation:

$$J = \int_0^T \left(\left(y - y_r\right)^2 + Ru^2\right) dt, \tag{12}$$

where y is the measured engine speed and y_r is the reference engine speed from the rigid vehicle model. Because the rising time in the tip-in process is always less than 0.1 s, the terminal time T of the cost function is set to 0.1 in order to guarantee the dynamic response. Definitely, T can be set to other values according to the dynamic response demand but out of the consideration in this study. The vehicle dynamic response is assumed to be good if the engine speed can quickly track the reference value. By minimizing the cost function in a standard form, the output u can be obtained by the following equation:

$$u = -KX + R^{-1}B^T g, \tag{13}$$

where $K = R^{-1}B^T P$. P is obtained by solving the Riccati equation shown as

$$\dot{P} = -PA - A^{\mathrm{T}}P + PBR^{-1}B^{\mathrm{T}}P - C_{\mathrm{T}}^{\mathrm{T}}QC_{\mathrm{T}}, \tag{14}$$

where g is obtained by

$$\dot{g} = \left[PBR^{-1}B^{\mathrm{T}} - A^{\mathrm{T}}\right]g - C_{\mathrm{T}}^{\mathrm{T}}Qz. \tag{15}$$

The boundary conditions are as follows:

$$\begin{aligned} P(t_{\mathrm{f}}) &= C_{\mathrm{T}}^{\mathrm{T}}F(t_{\mathrm{f}})C_{\mathrm{T}}, \\ g(t_{\mathrm{f}}) &= C_{\mathrm{T}}^{\mathrm{T}}F(t_{\mathrm{f}})z, \end{aligned} \tag{16}$$

where $t_{\mathrm{f}} = 0.1$ s, $F(t_{\mathrm{f}})$ is the terminal cost matrix, and z is the reference engine speed at the time t_{f} calculated by the reference vehicle model.

3.3. Comparison of Performances. A closed-loop simulation environment is built by connecting the MATLAB/Simulink-based controller and the ADAMS-based three-dimensional vehicle model. The simulations are conducted in a tip-in process with torque change from 0 to 80 Nm within 0.1 s, shown in Figure 3.

The simulation results without control, with LQR control, and with LQT control are compared, shown in Figures 4 and 5.

Figure 4 shows that the engine output torque under the LQT-based speed tracking control rises much faster than that under the LQR-based torque regulator control. Therefore, the LQT-based control is able to get a faster dynamic response. Nonetheless, it has an obvious torque fluctuation, which is eliminated under the LQR-based torque regulator control. As a result, the acceleration under the LQR control reaches the stable level faster than that under the LQT control but with the disadvantage of a slower dynamic response as shown in Figure 5. By a trial-and-error parameter tuning process for these two controllers, it can be concluded that a faster dynamic response with less overshoot cannot be met simultaneously under the LQT- or LQR-based control. The torque rising phase and torque holding phase should be considered separately for controller design.

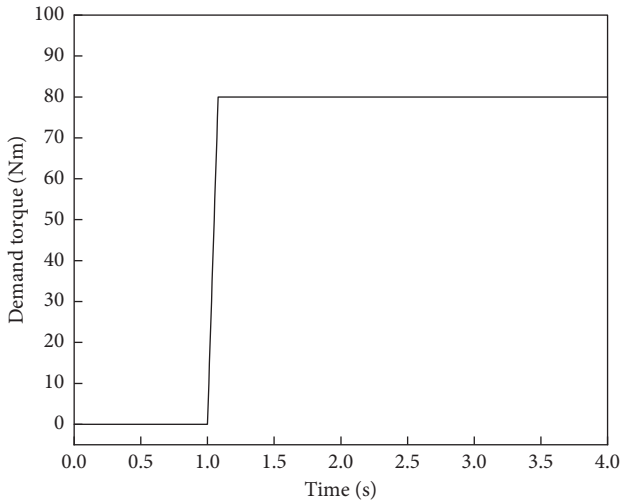

Figure 3: Demand torque change in the tip-in process.

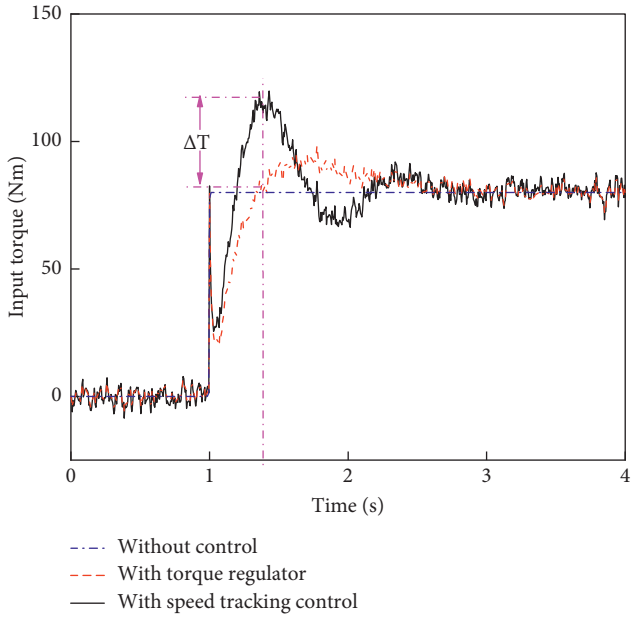

Figure 4: Engine torque with different control strategies.

4. Fuzzy Switching Control Design

In the above analysis, the speed tracking control is able to get faster dynamic response in the tip-in process than that of the torque regulator control. Considering the demands of the quick response in the torque rising phase and less fluctuation in the torque holding phase, the two controllers should work in the two phases separately. In this case, the LQR-based torque regulator control works in the torque holding phase whereas LQT-based speed tracking control works in the torque rising phase. However, the two controllers working in sequence introduce new problems. One is when to switch to another controller to guarantee optimal performances in both of the two phases separately. Another problem is how to make the output torque of the two controllers switching smoothly without any torque gaps and oscillations. The next two parts show the solution of the two problems.

4.1. Fusion Mechanism. A typical tip-in process without any oscillation controls applied is shown in Figure 6.

Figure 6 shows that the acceleration vibration occurs when it crosses over the steady-state value. Therefore, with the target of reducing this vibration, it is reasonable to set the steady-state value of acceleration as a threshold. With this definition, the controller switching time can be set to the time when the real-time acceleration reaches the threshold for the first time in the tip-in process. Before the switching time, the LQT-based speed tracking controller is applied to ensure a fast dynamic response whereas after the switching time, the LQR-based torque regulator controller is used to suppress the acceleration oscillation. In this case, we can get fast response in the torque rising phase and less fluctuation in the torque holding phase. However, the deviation of the two controllers at the switching time leads to a torque gap

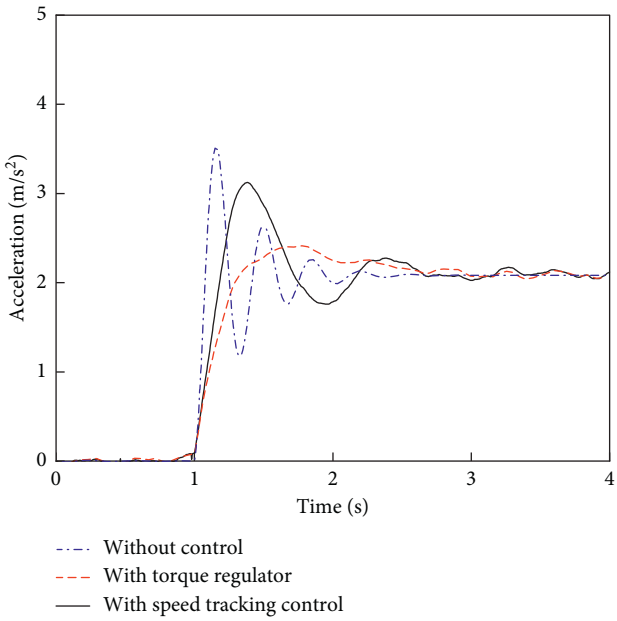

Figure 5: Vehicle longitudinal acceleration.

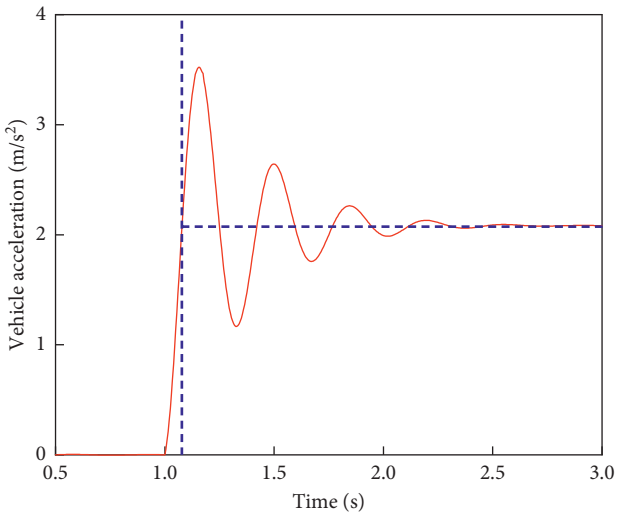

Figure 6: Acceleration without vibration control.

which introduces extra driveline vibration and vehicle longitudinal vibration, shown in Figure 4. It shows that the engine torque calculated from the LQR control is inconsistent with that from the LQT control, which introduces a torque gap ΔT. Consequently, the two controllers should be fused with a smooth switch. Here, a fuzzy-based fusion method with respect to the dynamic response and comfort is proposed to switch the torque smoothly.

4.2. Fusion Structure. A fusion coefficient λ is introduced for smooth torque switching. Then, the final engine torque is calculated by the following equation:

$$u = \lambda \cdot u_{\mathrm{T}} + (1 - \lambda) \cdot u_{\mathrm{R}}, \tag{17}$$

where u_{R} is the output of the LQR, and u_{T} is the output of the LQT. λ is in the interval [0,1]. The key concept is how to determine the fusion coefficient λ in order to eliminate the torque gap but without introducing extra driveline vibration. Therefore, a fusion method based on fuzzy logic theory is proposed to get the ideal value of the fusion coefficient λ. Combined with the LQR and LQT controls, the overall fusion structure is shown in Figure 7.

During the tip-in process, λ is updated in real time based on the proposed fusion algorithm. Considering different goals in the two phases, λ should be relatively large in the torque rising phase to guarantee the dynamic response whereas λ should be relatively small in the torque holding phase to ensure less oscillation. Therefore, a smooth change from large value to small value of λ is required for the proposed fusion algorithm which is able to guarantee a smooth torque switching process.

4.3. Input Signals. From the above part, we know the trend of λ in tip-in process but a precise trajectory of λ is still needed. To obtain that trajectory, a precise relationship between λ and the performances, such as dynamic response and less vibration in that case, is needed. Then, λ is tuned with respect to the relationship, and this process will be achieved automatically by the proposed fuzzy fusion method. Therefore, certain signals from the sensors on the vehicle or the CAN bus, which have the characteristics of the required performances, should be selected as the inputs of the proposed fuzzy algorithm. In this case, the proposed fuzzy algorithm is able to use these specific signals to calculate the desired value of λ satisfying the performance demand. Normally, three signals are chosen to represent the dual performances mentioned above: dynamic response and comfort. The absolute value of the difference ($\Delta\omega$) between the engine speed and wheel speed is able to predict the low-frequency vibration. The absolute value of the changing rate of the demand torque (T) is able to reflect the dynamic response. The absolute value of the difference ($\Delta\omega_{\mathrm{r}}$) between the actual engine speed and the reference engine speed is able to predict both of the dynamic response and the vibration. In a certain tip-in process, comparison of the three signals with a same scale is shown in Figure 8.

From Figure 8, it can be seen that the trends of $\Delta\omega$ and $\Delta\omega_{\mathrm{r}}$ are similar in frequency whereas $\dot{T}_{\mathrm{e}}$ has different trends from the other two. Therefore, $\Delta\omega$ and $\dot{T}_{\mathrm{e}}$ are chosen as inputs of the proposed fuzzy fusion algorithm. The input variables of the fuzzy fusion algorithm can be written as

$$\begin{aligned} \Delta\omega(n) &= \left| \frac{\dot{\theta}_1(n)}{i} - \dot{\theta}_2(n) \right|, \\ \dot{T}_{\mathrm{e}}(n) &= \left| \frac{\dot{T}}{4000} \right| = \left| \frac{(T(n)) - T(n-1)}{4000 \times \Delta t} \right|. \end{aligned} \tag{18}$$

4.4. Fuzzy Logic. To design an effective fuzzy logic algorithm, input and output fuzzy sets also need to be defined [20]. They

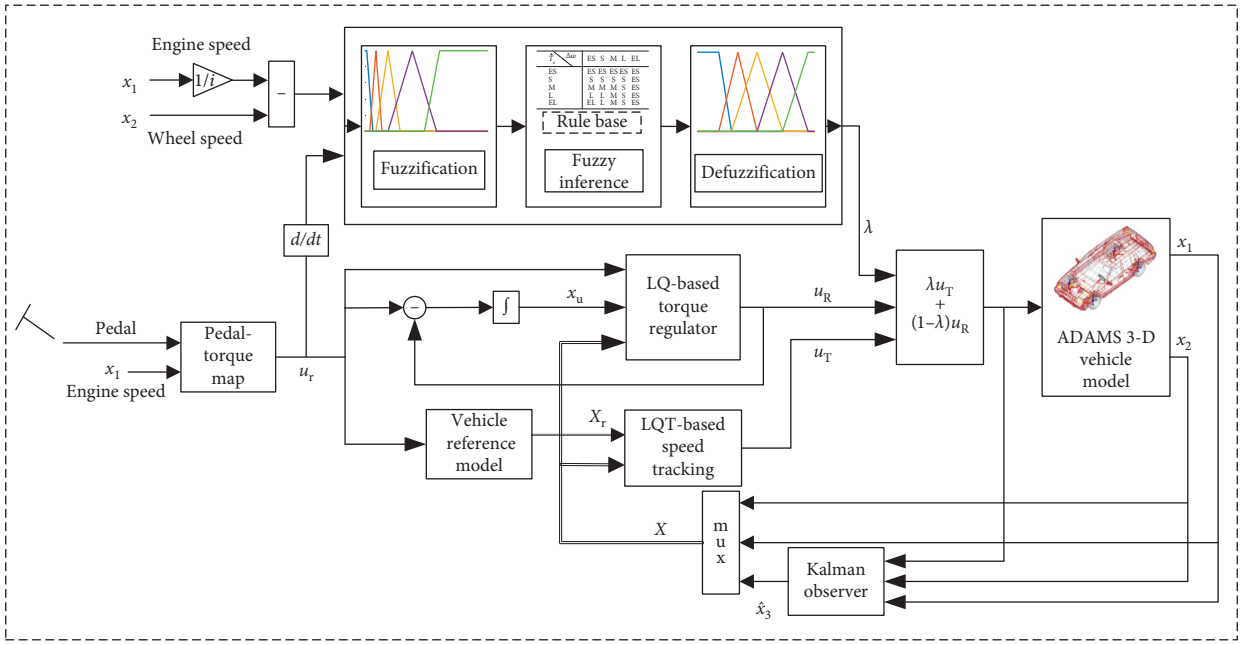

Figure 7: Fuzzy switching control structure.

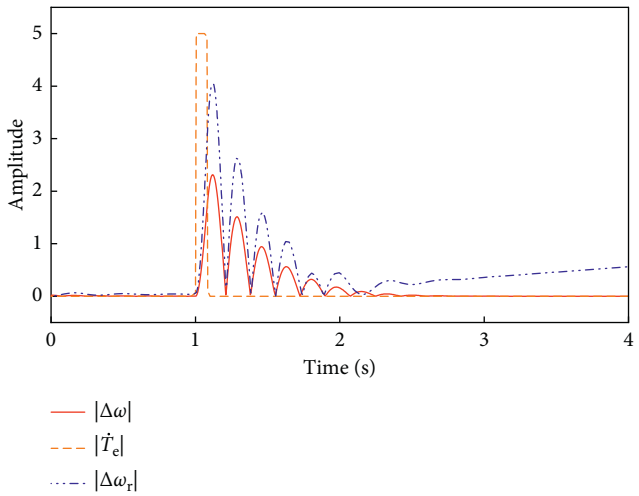

Figure 8: Acceleration without vibration control.

are presented in the fuzzification step following with fuzzy rules and defuzzification.

4.4.1. Fuzzification. Fuzzification makes the controller inputs dimensionally compatible with the conditions of the knowledge-based rules by using suitable linguistic variables. To provide a sufficient number of rules, 5 linguistic terms are used for both the inputs and output, which are defined as follows:

$$\begin{aligned} \Delta\omega(n) &= \{\text{ES, S, M, L, EL}\}, \\ \dot{T}_e(n) &= \{\text{ES, S, M, L, EL}\}, \\ \lambda &= \{\text{ES, S, M, L, EL}\}. \end{aligned} \tag{19}$$

The linguistic terms are listed and explained in Table 1. The input fuzzy sets membership functions for $\Delta\omega(n)$ and $\dot{T}_e(n)$ are shown in Figures 9(a) and 9(b). The output fuzzy sets membership functions are shown in Figure 9(c).

Table 1: Linguistic terms.

Index	Representation
ES	Extremely small
S	Small
M	Medium
L	Large
EL	Extremely large

4.4.2. Fuzzy Rules. Fuzzy rules are used to control the output variables based on the inputs. In that case, typical rules are explained as follows:

(1) $\Delta\omega(n)$ is extremely small (ES), and $\dot{T}_e(n)$ is extremely large (EL). In that case, the demand engine torque rises rapidly without torque fluctuation. Therefore, the dynamic response of the vehicle is required. According to Equation (17), λ should be extremely large in order to output more intense torque calculated by the LQT. As a result, λ should be EL.

(2) $\Delta\omega(n)$ is extremely large (EL), and $\dot{T}_e(n)$ is extremely small (ES). In that case, the demand engine torque is stable whereas the driveline and vehicle body undergo strong vibration. The phenomenon also indicates that it is in the toque holding phase. Therefore, the reduction of the vibration is required sharply. As a result, λ should be extremely small in order to output more moderate torque calculated by the LQR, and λ should be ES.

All rules in the proposed fuzzy algorithm are listed in Table 2.

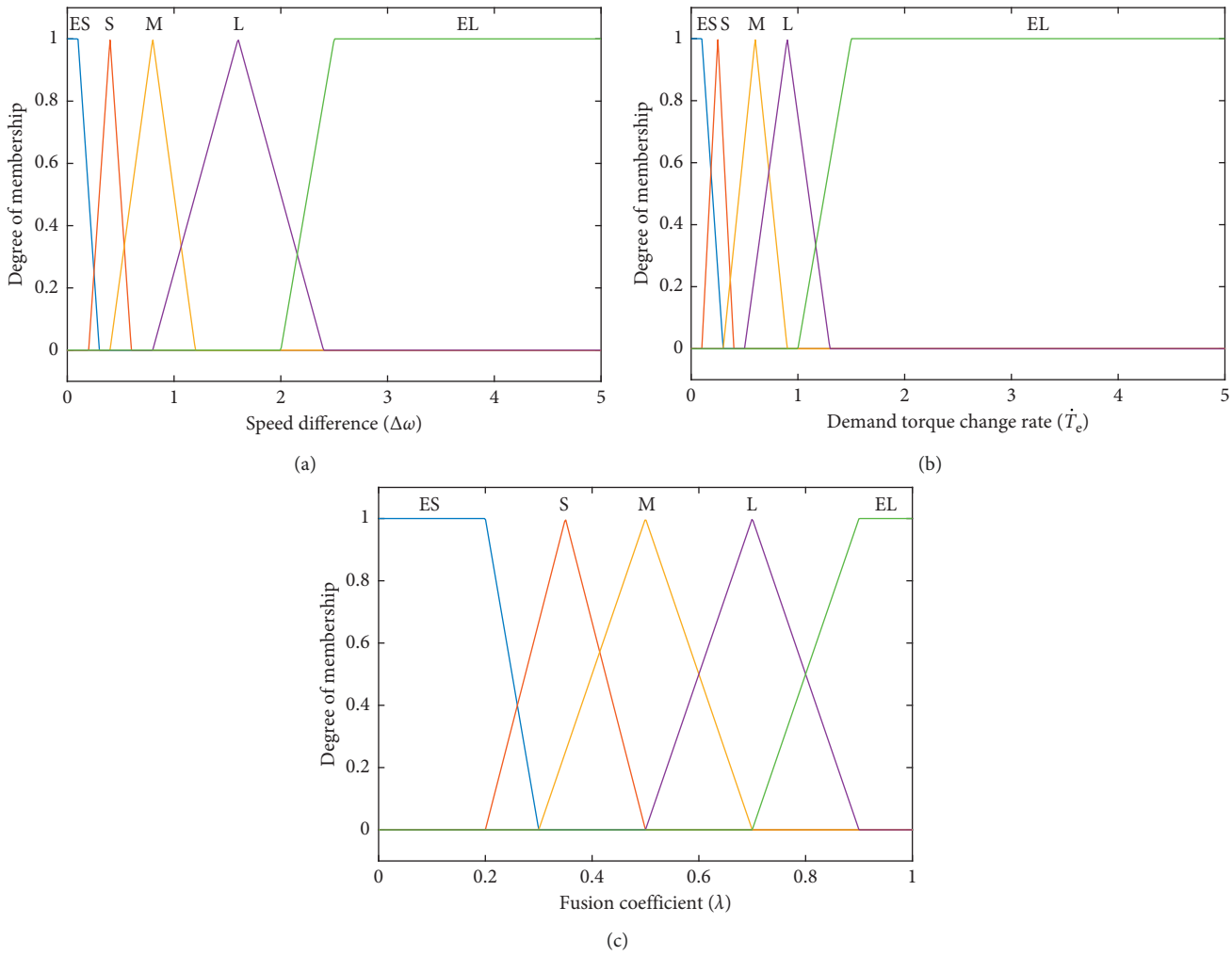

Figure 9: Membership functions of input and output variables. (a) Membership functions of $\Delta\omega(n)$. (b) Membership functions of $\dot{T}_e(n)$. (c) Membership functions of λ.

Table 2: Fuzzy rules.

$\dot{T}_e$	$\Delta\omega$				
	ES	S	M	L	EL
S	ES	ES	ES	ES	ES
S	S	S	S	S	ES
M	M	M	M	S	ES
L	L	L	M	S	ES
EL	EL	L	M	S	ES

4.4.3. Defuzzification. By using the fuzzy rules shown in Table 2, a fuzzy result can be obtained. But it cannot be used as the controller output directly. This fuzzy result should be defuzzified to obtain a final crisp output. Defuzzification is performed according to the membership functions of the output variable shown in Figure 9(c). The center of mass technique is used to find the center of mass of the output distribution in order to come up with one crisp number as the controller output [21]. Here, we chose a discrete calculation method for the center of mass defuzzification technique. It is computed as follows:

$$\lambda = \frac{\sum_{j=1}^{q} z_j u_{\underset{\sim}{C}}(z_j)}{\sum_{j=1}^{q} u_{\underset{\sim}{C}}(z_j)}. \tag{20}$$

Output λ is the center of mass and $u_{\underset{\sim}{C}}$ is the membership in class $\underset{\sim}{C}$ at the value z_j.

Besides, to effectively control the system, the range related to different variables should be calibrated through simulations or experiments. As shown in Figure 8, the ranges of the two input variables are set to [0, 5].

5. Results

A closed-loop simulation environment is built by connecting the MATLAB/Simulink-based controller and the ADAMS-based three-dimensional vehicle model. The demand torque increases from 0 to 80 Nm within 0.1 s which is the same with that in the section "Performance comparison." During the simulation, the LQR, LQT, and fuzzy-based switching control are running simultaneously. The fusion coefficient λ is calculated by the fuzzy fusion

algorithm in real time, thus changes with time, shown in Figure 10.

Note that after 1 s, λ gradually decreases from 0.9 to 0.1, which indicates a smooth switching from the LQT control to the LQR control. With the change of λ, the final output torque is calculated by Equation (17), and the variation is shown in Figure 11.

Figure 11 shows that the abrupt change of the demand torque is eliminated and the final engine output torque grows smoothly in the tip-in process. The simulation results with the LQR, LQT, and fuzzy switching controls are illustrated in Figures 12 and 13.

From Figures 12 and 13, it can be seen that fuzzy-based switching control achieves a better trade-off between the LQR and LQT, which makes a satisfying comfort and dynamic response.

To quantitatively evaluate the performances of the three controllers, an evaluation method considering the comfort and dynamic should be established. $\Delta\omega(n)$ is a reasonable indicator for the driving comfort but it does not allow a reliable and objective evaluation due to the vehicle's suspension and the subjective impression of the driver. Hence, an objective comfort evaluation algorithm is implemented using the longitudinal acceleration measured at the driver's cabin [22]. This method uses the error of the maximum and minimum acceleration as an important factor to represent the energy or the amplitude of the oscillation only when the derivate of the acceleration is below zero. The comfort evaluation index is calculated by

$$P_c = \frac{1}{T}\sum_{i=1}^{N}\left[s(t)\left(\max_{\dot{a}<0} a(t) - \min_{\dot{a}<0} a(t)\right)_i\right], \tag{21}$$

where $a(t)$ is the longitudinal acceleration measured at the driver's cabin, the weighting $s(t)$ is increasing with time, T is the total duration of the acceleration derivate in negative direction, and N is the number of the acceleration derivate from positive direction to negative direction. The higher is the P_c, the worse the comfort is.

The dynamic performance is evaluated by the rising time of the longitudinal acceleration from the origin to its stable value. By using the simulation data and the evaluation method, the quantitative evaluation results are listed in Table 3.

Table 3 shows that the comfort index of the fuzzy-based switching control is improved by 96.78% compared with that of the uncontrolled situation. More importantly, the comfort index of the fuzzy-based switching control improves by 79.74% compared with that of the LQT-controlled condition but the dynamic response time only increases by 24%. Besides, compared with the LQR-controlled condition, the dynamic response time improved by 21.88% with only 9.68% deterioration in the comfort index. Above all, the proposed fuzzy-based switching control utilizes the advantages of both the LQR and LQT-based controls while diminishes their disadvantages.

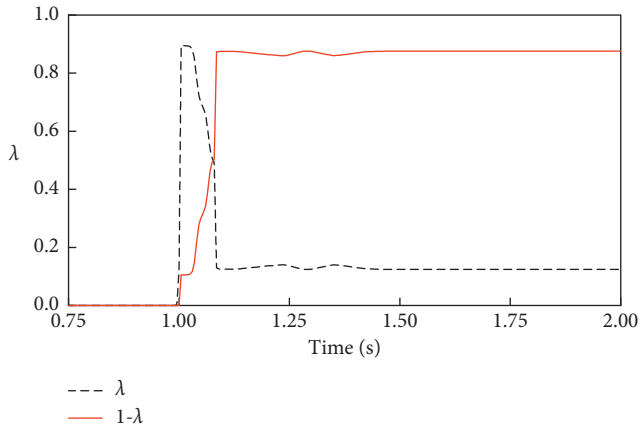

Figure 10: Coefficient λ and the complement $1-\lambda$ in tip-in process.

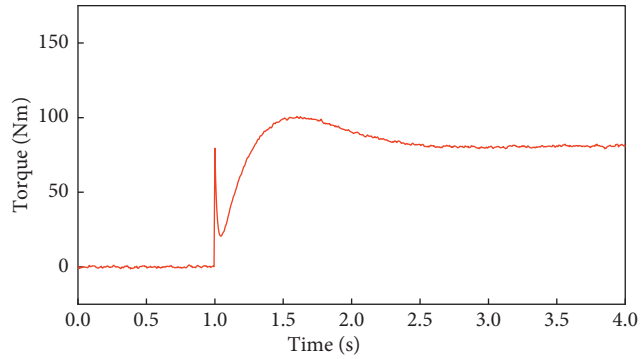

Figure 11: The final output torque with fuzzy switching control.

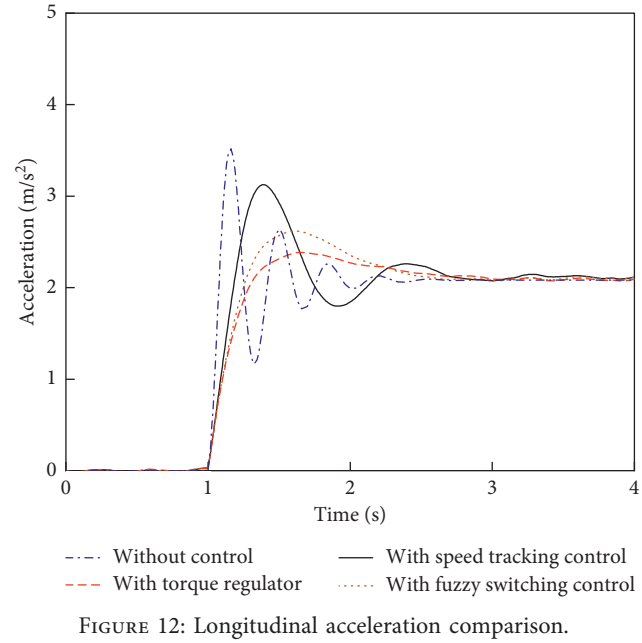

Figure 12: Longitudinal acceleration comparison.

6. Conclusion

A sudden change in the engine torque causes torsional vibration of the driveline, resulting in fluctuation in the driving torque of the wheel, which in turn introduces low-frequency vibration in vehicle longitudinal direction. Traditionally, LQ-based controllers are used to suppress that vibration by compensating additional torque to the original

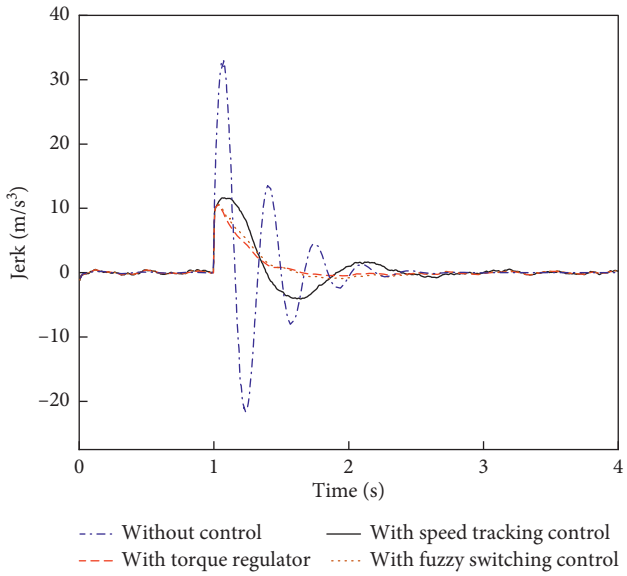

Figure 13: Derivative of acceleration (jerk) comparison.

Table 3: Evaluation of vehicle comfort and dynamic response with the proposed controls.

	Comfort index	Dynamic response (s)
Without control	9.64	0.08
With LQR	0.28	0.32
With LQT	1.53	0.19
With fuzzy switching control	0.31	0.25

system. From the study and comparison, it can be seen that LQR-based torque regulator control has a good comfort performance in reducing vibration whereas the LQT-based speed tracking control has a good dynamic response but with overshoot and vibration. These two types of controllers are not able to guarantee both comfort and dynamic response in the whole tip-in process.

This paper has presented a novel control method in the automotive field to suppress the vibration with good comfort and dynamic response simultaneously. The proposed fuzzy-based switching control strategy determines the fusion coefficient of the LQR and LQT-based controllers in torque rising and holding phases. This strategy uses the increasing rate of the demand torque and the difference between engine speed and wheel speed as inputs to predict both of the dynamic response and the vibration. Then, the designed fuzzy rules and fuzzy membership functions output the desired fusion coefficient. By combining the torque calculated by the LQR and LQT with the fusion coefficient, the final engine output torque is obtained. The simulation results show that fuzzy-based switching control outputs smooth demand engine torque which is able to achieve a better trade-off between the LQR and LQT controls to makes a satisfying comfortability and dynamic response. Through a quantitative comfortability and dynamic response evaluation method, the comfortability index of the fuzzy-based switching control improves by 79.74% compared with that of the LQT-controlled condition and the dynamic response time improved by 21.88% compared with that of the LQR-controlled condition. As a summary, the proposed fuzzy switching control strategy is able to suppress the low-frequency longitudinal vibration with a satisfying dynamic response and comfortability.

Table 4: Main parameters of the vehicle.

Symbol	Value
Vehicle mass	1420 kg
Clutch torsional stiffness	60 Nm/rad
Clutch torsional damping	5 Nm/(rad/s)
Halfshaft torsional stiffness	5260 Nm/rad
Halfshaft torsional damping	10 Nm/(rad/s)
Tire torsional stiffness	7000 Nm/rad
Tire torsional damping	2.5 Nm/rad
Suspension stiffness	90000 N/(m/s)
Rear suspension damping	3000 N/(m/s)
Gearbox ratio	3.308
Rear differential ratio	4.158
Engine flywheel inertia	0.11 kgm^2
Clutch inertia	0.05 kgm^2
Wheel inertia	1.8 kgm^2
Wheel radius	0.33 m
Wheelbase	2.7 m

Appendix

A. Main Parameters of the Vehicle

A list of the main parameters of the vehicle is given in Table 4.

B. Values of the State-Space Formulation Matrices

Each element value of the matrices of the state-space formulation is shown here:

$$A = \begin{bmatrix} -3.78 & 52.02 & -3.24 \\ 0.04 & -0.59 & 36.91 \\ 0.07 & -1 & 0 \end{bmatrix},$$
$$B = \begin{bmatrix} 5.95 & 0 & 0 \end{bmatrix}^{\mathrm{T}}, \quad \text{(B.1)}$$
$$C_{\mathrm{R}} = \begin{bmatrix} -4.37 & 60.12 & -3744 \end{bmatrix}.$$

Data Availability

The data used to support the findings of this study are included within the article.

Conflicts of Interest

The authors declare that they have no conflicts of interest.

Acknowledgments

The authors would like to acknowledge the National Natural Science Foundation of China for financially supporting this

research under Project nos. 51475043 and 50975026. Also, the authors would like to thank Yu Zhang, Shuailin Zhang, and Yinan Rong from the Beijing Hyundai Motor Company, who provided the test vehicle and parameters for our research.

References

[1] A. Sorniotti, "Driveline modeling, experimental validation and evaluation of the influence of the different parameters on the overall system dynamics," Technical Report, SAE Technical Paper, 2008.

[2] E. Rabeih and D. Crolla, "Coupling of driveline and body vibrations in trucks," Technical Report, SAE Technical Paper, 1996.

[3] Y. Choi, H. Song, J. Lee, and H. Cho, "An experimental study for drivability improvements in vehicle acceleration mode," *Proceedings of the Institution of Mechanical Engineers, Part D: Journal of Automobile Engineering*, vol. 217, no. 7, pp. 623–631, 2003.

[4] K. Park, J. Lee, and J. Park, "Torque control of a vehicle with electronic throttle control using an input shaping method," *International Journal of Automotive Technology*, vol. 14, no. 2, pp. 189–194, 2013.

[5] J. Fredriksson, H. Weiefors, and B. Egardt, "Powertrain control for active damping of driveline oscillations," *Vehicle System Dynamics*, vol. 37, no. 5, pp. 359–376, 2002.

[6] S. Richard, P. Chevrel, and B. Maillard, "Active control of future vehicles drivelines," in *Proceedings of 38th IEEE Conference on Decision and Control*, pp. 3752–3757, IEEE, Phoenix, AZ, USA, December 1999.

[7] P. Templin and B. Egardt, "An lqr torque compensator for driveline oscillation damping," in *Proceedings of 2009 IEEE International Conference on Control Applications*, pp. 352–356, IEEE, Riverside CA, USA, July 2009.

[8] M. Bruce, B. Egardt, and S. Pettersson, "On powertrain oscillation damping using feedforward and lq feedback control," in *Proceedings of 2005 IEEE Conference on Control Applications CCA 2005*, pp. 1415–1420, IEEE, Toronto, ON, USA, August 2005.

[9] C. Fang, Z. Cao, M. M. Ektesabi, A. Kapoor, and A. Sayem, "Model reference control for active driveability improvement," in *Proceedings of 2014 6th International Conference on Modelling, Identification and Control (ICMIC)*, pp. 202–206, IEEE, Melbourne, Australia, December 2014.

[10] A. Lagerberg and B. Egardt, "Model predictive control of automotive powertrains with backlash," *IFAC Proceedings Volumes*, vol. 38, no. 1, pp. 1–6, 2005.

[11] J. Baumann, D. D. Torkzadeh, A. Ramstein, U. Kiencke, and T. Schlegl, "Model-based predictive anti-jerk control," *Control Engineering Practice*, vol. 14, no. 3, pp. 259–266, 2006.

[12] J. Baumann, A. Swarnakar, U. Kiencke, and T. Schlegl, "A robust controller design for anti-jerking," Technical Report, SAE Technical Paper, 2005.

[13] D. Hao, C. Zhao, and Y. Huang, "A reduced-order model for active suppression control of vehicle longitudinal low-frequency vibration," *Shock and Vibration*, vol. 2018, Article ID 5731347, 22 pages, 2018.

[14] L. Castellazzi, A. Tonoli, N. Amati, and E. Galliera, "A study on the role of powertrain system dynamics on vehicle driveability," *Vehicle system dynamics*, vol. 55, no. 7, pp. 1012–1028, 2017.

[15] O. Atabay, M. Ötkür, and İ. M. Ereke, "Model based predictive engine torque control for improved drivability," *Proceedings of the Institution of Mechanical Engineers, Part D: Journal of Automobile Engineering*, vol. 232, no. 12, pp. 1654–1666, 2017.

[16] C. F. Caruntu, A. E. Balau, M. Lazar, P. van den Bosch, and S. Di Cairano, "A predictive control solution for driveline oscillations damping," in *Proceedings of the 14th International Conference on Hybrid Systems: Computation and Control*, pp. 181–190, ACM, Berlin, Germany, April 2014.

[17] P. Templin and B. Egardt, "A powertrain lqr-torque compensator with backlash handling," *Oil and Gas Science and Technology–Revue dIFP Energies nouvelles*, vol. 66, no. 4, pp. 645–654, 2011.

[18] F. U. Syed, M. L. Kuang, and H. Ying, "Active damping wheel-torque control system to reduce driveline oscillations in a power-split hybrid electric vehicle," *IEEE Transactions on Vehicular Technology*, vol. 58, no. 9, pp. 4769–4785, 2009.

[19] A. E. Bălău, *Overall Powertrain Modeling and Control based on Driveline Subsystems Integration (controlul integrat al lanÈ›ului de transmisie a puterii)*, Universităţii Tehnice din Cluj-Napoca, Cluj-Napoca, Romania, 2011.

[20] H. Ying, *Fuzzy Control and Modeling: Analytical Foundations and Applications*, Wiley-IEEE Press, Hoboken NJ, USA, 2000.

[21] T. J. Ross, *Fuzzy Logic with Engineering Applications*, John Wiley & Sons, Hoboken NJ, USA, 2005.

[22] L. Webersinke, D. Feth, M. Hertweck, A. von Vietinghoff, and U. Kiencke, "Optimization of heavy truck's driveline performance via model predictive control rated by a comfort evaluation algorithm," *IFAC Proceedings Volumes*, vol. 41, no. 2, pp. 7058–7063, 2008.